THE JOURNAL OF BIOLOGICAL CHEMISTRY VOL. 283, NO. 11, pp. 7100–7108, March 14, 2008

Conopressin-T from *Conus tulipa* Reveals an Antagonist Switch in Vasopressin-like Peptides*[S]

Received for publication, August 6, 2007, and in revised form, December 14, 2007 Published, JBC Papers in Press, January 2, 2008, DOI 10.1074/jbc.M706477200

Sébastien Dutertre[‡1], Daniel Croker[§], Norelle L. Daly[‡], Åsa Andersson[§], Markus Muttenthaler[‡], Natalie G. Lumsden[‡], David J. Craik[‡], Paul F. Alewood[‡], Gilles Guillon[¶‖‡‡], and Richard J. Lewis[‡2]**

*From the [‡]Institute for Molecular Bioscience, University of Queensland, Brisbane, Queensland 4072, Australia, [§]Xenome Ltd., Brisbane, Queensland 4072, Australia, and the [¶]Institut de Génomique Fonctionnelle, Département d'Endocrinologie, [‖]CNRS UMR 5203, and **INSERM U661, [‡‡]Université Montpellier I et II, Montpellier F-34094, France*

We report the discovery of conopressin-T, a novel bioactive peptide isolated from *Conus tulipa* venom. Conopressin-T belongs to the vasopressin-like peptide family and displays high sequence homology to the mammalian hormone oxytocin (OT) and to vasotocin, the endogenous vasopressin analogue found in teleost fish, the cone snail's prey. Conopressin-T was found to act as a selective antagonist at the human V_{1a} receptor. All peptides in this family contain two conserved amino acids within the exocyclic tripeptide (Pro^7 and Gly^9), which are replaced with Leu^7 and Val^9 in conopressin-T. Whereas conopressin-T binds only to OT and V_{1a} receptors, an L7P analogue had increased affinity for the V_{1a} receptor and weak V_2 receptor binding. Surprisingly, replacing Gly^9 with Val^9 in OT and vasopressin revealed that this position can function as an agonist/antagonist switch at the V_{1a} receptor. NMR structures of both conopressin-T and L7P analogue revealed a marked difference in the orientation of the exocyclic tripeptide that may serve as templates for the design of novel ligands with enhanced affinity for the V_{1a} receptor.

The vasopressin (AVP)[3] and oxytocin (OT) peptides were originally discovered and identified as neurohypophysial hormones in mammals (1). In humans, AVP acts via three vasopressin receptors (vascular $V_{1a}R$, pituitary $V_{1b}R$, and renal V_2R), whereas OT acts via one OT receptor (OTR). All targets are members of the G protein-coupled receptor family (2). Peripherally, they regulate water balance, the control of blood pressure, and contraction of uterine smooth muscle and mammary myoepithelium (3). Centrally, these peptides affect levels of aggression, depression, and young parent bonding (4–6). Endogenous analogues of OT and AVP have been reported in nonmammalian vertebrates, annelids, molluscs, and insects, suggesting an old lineage for these peptides (7). Surprisingly, two variants were also found in the venom of predatory cone snails. The original discovery of these two AVP analogues, named conopressins, was based on the characteristic "scratching" effect observed upon intracerebral injection into mice (8). Although the sequences of conopressins are similar to vasopressin itself, they have an additional positive charge in position 4, which is only found in two other endogenous vasopressin analogues, cephalotocin (*Octopus vulgaris*) and annetocin (*Eisenia foetida*). Conopressin-S was isolated from *Conus striatus*, whereas conopressin-G was first isolated from *Conus geographus* venom but later found in *Conus imperialis* venom as well as in tissue extracts of the nonvenomous snails *Lymnea stagnalis* and *Aplysia californica* and the leech *Erpobdella octoculata* (9–11).

Molluscs of the genus *Conus* produce bioactive peptides in a combinatorial fashion. As demonstrated for the snake toxins (12), most conotoxins or conopeptides are believed to be derived from an endogenous structural template (13). Because conopressin-G is widely distributed, it may represent the endogenous hormone in Gastropods and Annelids. However, a role in prey capture has also been proposed (14).

In this study, we report the discovery of conopressin-T isolated from *Conus tulipa* venom. Pharmacological characterizations of Con-T across human receptors revealed that it is a selective V_{1a} antagonist, with partial agonist activity at the OT receptor and no detectable activity at V_{1b} and V_2 receptors. The exocyclic tripeptide segment of conopressin-T shows unusual sequence divergence. L7P-Con-T had increased affinity at the V_{1a} receptor but minimal effect on the selectivity profile across all human receptors compared with Con-T. Interestingly, replacing Gly^9 with Val^9 in OT and AVP converted these peptides from full agonist to full antagonist at the V_{1a} receptor, demonstrating the role of position 9 as an antagonist switch in these peptides. Finally, the NMR structures of conopressin-T and its L7P analogue provide new templates for the design of novel pharmacological agents with enhanced activity at the V_{1a} receptor.

* This work was supported by a postgraduate scholarship from the University of Queensland (to S. D.), a Discovery Grant from the Australian Research Council (to R. J. L., P. F. A., and D. J. C.), and an NHMRC Program Grant (to R. J. L. and P. F. A.). The costs of publication of this article were defrayed in part by the payment of page charges. This article must therefore be hereby marked "*advertisement*" in accordance with 18 U.S.C. Section 1734 solely to indicate this fact.

[S] The on-line version of this article (available at http://www.jbc.org) contains supplemental Figs. 1 and 2.

[1] Recipient of a long-term EMBO postdoctoral fellowship. Present address: Max Planck Institute for Brain Research, Department of Neurochemistry, 46 Deutschordenstrasse, 60529 Frankfurt, Germany.

[2] To whom correspondence should be addressed: Institute for Molecular Bioscience, University of Queensland, Brisbane, Queensland 4072, Australia. Tel.: 61-7-3346-2984; Fax: 61-7-3346-2101; E-mail: r.lewis@imb.uq.edu.au.

[3] The abbreviations used are: AVP, vasopressin; AVT, vasotocin; Con-S, conopressin-S; Con-T, conopressin-T; IP, total inositol phosphate; OT, oxytocin; OTR, OT receptor; HPLC, high pressure liquid chromatography; RP, reversed phase; CHO, Chinese hamster ovary; GPCR, G protein-coupled receptor; MS, mass spectrometry.

EXPERIMENTAL PROCEDURES

Materials—*t*-Butoxycarbonyl-protected amino acids and reagents used during chain assembly and HPLC purification (dimethylformamide, dichloromethane, acetonitrile, and trifluoroacetic acid) were peptide synthesis grade purchased from Auspep (Melbourne, Australia) and Novabiochem (San Diego, CA). 4-methylbenzhydrylamine-NH_2 resin was obtained from Applied Biosystems (Foster City, CA). Most standard chemicals were purchased from Sigma, Roche Applied Science, or Merck, unless otherwise indicated. AVP and OT came from Bachem (Bubendorf, Switzerland), and fetal calf serum was from Sigma. Myo-[2-^{3}H]inositol was from PerkinElmer Life Sciences. Minimal essential medium and Dulbecco's modified Eagle's medium were purchased from Invitrogen, and inositol-free Dulbecco's modified Eagle's medium came from ICN Biochemicals (Orsay, France). Dowex AG1-X8 formate form 200–400 mesh was purchased from Bio-Rad.

Human V_{1a} and V_{1b} MTS membranes from HEK293 cells, human V_2 MTS membranes from CHO-K1 cells, [^{3}H]OT ([tyrosyl-2,6-^{3}H]oxytocin; 40 Ci/mmol), ^{125}I-linear vasopressin V1a receptor antagonist ([^{125}I]phenylacetyl-DTyr(Me)-Phe-Gln-Asn-Arg-Pro-Arg-Tyr-NH_2; 2,200 Ci/mmol), [^{3}H]AVP ([Arg^8,tyrosyl-3,5-^{3}H]vasopressin; 19.4 Ci/mmol), FlashBlue™ GPCR scintillation beads, Betaplate Scintillant, GF/B filtermats, sample bags, and TopSeal-A 96-well plate sealing film were from PerkinElmer Life Sciences, [Arg^8]vasopressin from Auspep (Melbourne, Australia), Costar 96-well white polystyrene plates with clear flat bottoms from Corning Glass, pcDNA3.1/V5-His©TOPO®TA expression kit, ThermalAce™ DNA polymerase, SuperScript™ III RNase H-reverse transcriptase, Red hot TaqDNA polymerase, F-12 nutrient mixture (HAM) from Invitrogen, QuikChange™ XL site-directed mutagenesis kit from Stratagene (La Jolla, CA), human placenta total RNA from Ambion (Austin, TX), trypsin-Versene (EDTA), and Serum Supreme from Cambrex Biosciences (Walkersville, MD), all primers and oligonucleotides from Sigma, TransIT®-CHO transfection kit from Mirus (Madison, WI), and CHO-K1 cells from the American Tissue Culture Collection (Manassas, VA).

Isolation and Sequencing—Specimens of *Conus tulipa* were collected from the Great Barrier Reef, Australia. Venom ducts were dissected, and crude venom prepared as previously described (15). Initial fractionation of the venom was carried out by RP-HPLC, and fractions were stored at 4 °C until further use.

Conopressin-T was purified from fraction 30 using a 1% linear gradient of 0–60% solvent B in A over 60 min (A = 0.05% trifluoroacetic acid (aqueous); B = 0.045% trifluoroacetic acid, 90% acetonitrile) on an analytical C_{18} Phenomenex column. The flow rate was 1 ml/min, and the absorbance was monitored at 214 nm. N-terminal sequencing was carried out on an Applied Biosystems Procise HT Protein Sequencer (BRF, Newcastle, Australia) using ~20 pmol of purified peptide.

Peptide Synthesis—Conopressin-T and analogues were synthesized using the method described in Ref. 13, with minor modifications. Briefly, conopressin-T and L7P-conopressin-T were synthesized manually using *t*-butoxycarbonyl chemistry with *in situ* neutralization protocols (16) on a 0.5-mmol scale for residues 9 and 8. The peptide was then nitrogen-dried and split into two syntheses of 0.25 mmol for the remaining 7 residues of conopressin-T and L7P-conopressin-T. After HF cleavage, the crude peptides were purified by semipreparative RP-HPLC using a linear gradient of 0–60% B at 3 ml/min while monitoring UV absorbance at 214 nm. Air oxidation was carried out by dissolving 10 mg of the crude peptides in 45 ml of 0.1 M NH_4HCO_3 (pH 8.25) with vigorous stirring at room temperature for 1 h. Whereas L7P-conopressin-T dissolved readily at concentrations up to 0.5 mg/ml, conopressin-T was found to aggregate instantly. To overcome this, 1 mg of reduced conopressin-T was first dissolved in a 2:1 ratio of solution A and B and then slowly added to the oxidation buffer. Prior to purification, the solution was acidified to pH 3 with neat trifluoroacetic acid and analyzed by analytical C_{18} HPLC and electrospray-MS. Oxidized conopressin-T and L7P-conopressin-T were then purified by semipreparative RP-HPLC using the same chromatographic conditions as above. Pure fractions, as determined by analytical RP-HPLC and mass spectrometry, were pooled and lyophilized. Stock solutions of conopressin-T and L7P-conopressin-T were made in MilliQ water and quantified by analytical HPLC using a commercial AVP standard.

Cloning of Human OT Receptor—A 1.3-kb fragment of OT cDNA, containing the full coding region of the human OT receptor, was isolated from human placental cDNA constructed from total placental RNA using SuperScript™ III reverse transcriptase. The following forward (5′-GGTAGAG-GATTCCCGCTCATTTG-3′) and reverse (5′-GGGGAGG-GATACAAACTGATAGG-3′) primers were used to isolate the DNA fragment. This fragment was subcloned into the mammalian expression vector pcDNA3.1/V5-his-TOPO. Following sequence analysis, 8 nucleotide changes were found over the published OT sequence (NM_000916) encoding 7 amino acid changes with one change being conserved. The nucleotide changes were T47C, A281G, A256C, G532C, T646C, and A1121G, which correspond to amino acid changes of V16A, H73R, M86L, G178R, F216L, and N374S. These changes were mutated to the published sequence using a QuikChange™ XL site-directed mutagenesis kit.

OT Receptor Expression and Membrane Preparation—DNA was prepared and used for transfection in CHO-K1 cells. CHO-K1 cells were propagated in 150-mm plates with F-12 medium containing 10% Serum Supreme at 37 °C in a humidified atmosphere with 5% CO_2. Transient transfection was performed with an appropriate plasmid using the TransIT®-CHO transfection reagent method. Briefly, the method involved combining TransIT®-CHO reagent (72 μl) in serum-free F-12 medium incubated for 5 min at room temperature. Following the addition of receptor plasmid (24 μg), this mixture was incubated for 10 min at room temperature. CHO Mojo reagent (16 μl) was added to the mixture and incubated for 15 min at room temperature prior to the addition to the cells.

The transfected cells were harvested within 24 h by the following method. Confluent 150-mm plates were washed with phosphate-buffered saline (10 mM phosphate buffer, pH 7.4, 2.7 mM KCl, 137 mM NaCl), harvested by scraping into ice-cold harvest buffer (50 mM Tris-HCl, pH 7.4, 5 mM $MgCl_2$), followed

by homogenization with a Polytron homogenizer and centrifugation at 100 × *g* for 10 min at 4 °C. Supernatants were recovered and centrifuged at 22,000 × *g* for 1 h at 4 °C. Membrane pellets were resuspended in 0.5 ml of ice-cold assay buffer A (50 mM Tris-HCl, pH 7.4, 5 mM $MgCl_2$, 0.1% bovine serum albumin, containing 10% glycerol and aliquots stored at −80 °C until use.

Receptor Binding Studies—Receptor binding assays were performed using FlashBlue™ GPCR scintillation beads. FlashBlue™ GPCR beads are 3-μm polystyrene scintillating beads with wheat germ agglutinin covalently attached on the surface. These beads allow development of a homogeneous GPCR radioligand binding assay using cellular membranes. Briefly, FlashBlue™ GPCR SPA binding assays were performed in 96-well white polystyrene plates with clear flat bottoms (Costar). Radioligand (OTR [^{3}H]OT (2 nM), V_{1a} ^{125}I-labeled linear V_{1a} antagonist (21 pM), V_{1b} [^{3}H]AVP (0.5 nM), V_2 [^{3}H]AVP (0.85 nM)) was added to each membrane preparation, followed by the addition of various concentrations of competing compounds (1 pM to 10 μM) in a total volume of 80 μl containing assay buffer A or B (50 mM Tris-HCl, pH 7.4, 0.1% bovine serum albumin, and either 5 mM $MgCl_2$ (A) or 10 mM $MgCl_2$ (B)) (OT and V_2 assay, buffer A; V_{1a} and V_{1b} assay, buffer B). The final reaction volume per well comprised 20 μl of compound/buffer, 20 μl of FlashBlue™ GPCR beads (OTR, V_{1a}, and V_2, 100 μg; V_{1b}, 200 μg), and 20 μl of membrane, and the assay was initiated by the addition of 20 μl of radioligand. The plate was then sealed with TopSeal-A sealing film and incubated with shaking for 1 h at room temperature. Radioligand binding was then assessed for 30 s/well on a 1450 Microbeta scintillation counter (Wallac).

All binding data were analyzed using GraphPad PRISM (GraphPAD Software, Inc., San Diego, CA). Each data point was performed in triplicate and derived from at least three separate experiments. The inhibitory dissociation constant (K_i) was calculated using the following formula: $K_i = IC_{50}/(1 + [L]/K_d)$, where [L] is the concentration of radioligand present, and K_d is the dissociation constant of radioligand (17).

Inositol Phosphate Assays—Inositol phosphate accumulation was determined as previously described (18). Briefly, CHO cells stably transfected with AVP/OT receptors were plated at 100,000 cells/well. Cells were grown for 24 h in their respective culture medium (see above) and further incubated for another 24-h period in a serum- and inositol-free medium supplemented with 1 μCi·ml^{-1} myo-[2-^{3}H]inositol. Cells were then washed twice with Hanks' buffered saline medium, incubated for 15 min in this medium supplemented with 20 mM LiCl, and further stimulated for 15 min with increasing concentrations of analogues to be tested. The reaction was stopped by adding perchloric acid (5%, v/v). Total inositol phosphates (IPs) accumulated were extracted and purified on a Dowex AGI-X8 anion exchange chromatography column and counted.

NMR Spectroscopy—Samples for ^{1}H NMR measurements contained ~1 mM peptide in 95% H_2O, 5% D_2O (v/v) at pH ~3. Spectra were recorded at 290 K on a Bruker AVANCE-600 spectrometer. Two-dimensional NMR spectra were recorded in phase-sensitive mode using time-proportional phase incrementation for quadrature detection in the t1 dimension (19, 20). The two-dimensional experiments consisted of a TOCSY using a MLEV-17 spin lock sequence with a mixing time of 80 ms, DQF-COSY, and NOESY with mixing times of 200–300 ms. Solvent suppression was achieved using a modified WATERGATE sequence. Spectra were acquired over 6024 Hz with 4096 complex data points in F2 and 512 increments in the F1 dimension. $^3J_{HN\text{-}H\alpha}$ coupling constants were measured from a one-dimensional spectrum or from the DQF-COSY spectrum. Spectra were processed on a Silicon Graphics Indigo work station using XWINNMR (Bruker) software. The t1 dimension was zero-filled to 1024 real data points, and 90° phase-shifted sine bell window functions were applied prior to Fourier transformation.

Structure Calculations—Preliminary structures were calculated using a torsion angle simulated annealing protocol within the program DYANA (21). Final structures were calculated using simulated annealing and energy minimization protocols within CNS version 1.1 (22). The starting structures were generated using random (φ,ψ) dihedral angles and energy-minimized to produce structures with the correct local geometry. A set of 50 structures was generated by a torsion angle simulated annealing protocol (19, 20). This protocol involved a high temperature phase comprising 4000 steps of 0.015 ps of torsion angle dynamics, a cooling phase with 4000 steps of 0.015 ps of torsion angle dynamics during which the temperature was lowered to 0 K, and finally an energy minimization phase comprising 500 steps of Powell minimization. Structures consistent with restraints were subjected to further molecular dynamics and energy minimization in a water shell, as described by Linge and Nilges (23). The refinement in explicit water involved the following steps. First, heating to 500 K via steps of 100 K, each comprising 50 steps of 0.005 ps of Cartesian dynamics. Second, 2500 steps of 0.005 ps of Cartesian dynamics at 500 K before a cooling phase where the temperature was lowered in steps of 100 K, each comprising 2500 steps of 0.005 ps of Cartesian dynamics. Finally, the structures were minimized with 2000 steps of Powell minimization. Structures were analyzed using PROMOTIF (24) and PROCHECK-NMR (25).

RESULTS

Isolation and Sequencing of Conopressin-T—A peptide with a monoisotopic mass of 1107.54 Da was purified from *C. tulipa* venom (Fig. 1, *A–C*). The Tris(2-carboxyethyl)phosphine-reduced peptide displayed a mass of 1109.5 Da, suggesting the presence of one disulfide bond (data not shown). N-terminal sequencing produced the sequence CYIQNCLRV with a calculated mass of 1110.53 Da, consistent with one disulfide bond (−2 Da) and C-terminal amidation (−1 Da). A BLAST search revealed that this sequence belonged to the vasopressin peptide family characterized by a disulfide-containing ring (residues 1–6) and a short exocyclic C-terminal tripeptide (residues 7–9). Conopressin-T had 7 of 9 residues identical to vasotocin (AVT), including the first six residues also found in oxytocin and mesotocin, and Arg^8 known to be essential for the pressor activity in vasopressin. However, two highly conserved residues, Pro^7 and Gly^9, found in other vasopressin-like peptides as well as conopressin-G and conopressin-S are modified to Leu^7 and Val^9 in conopressin-T. *De novo* mass spectrometry

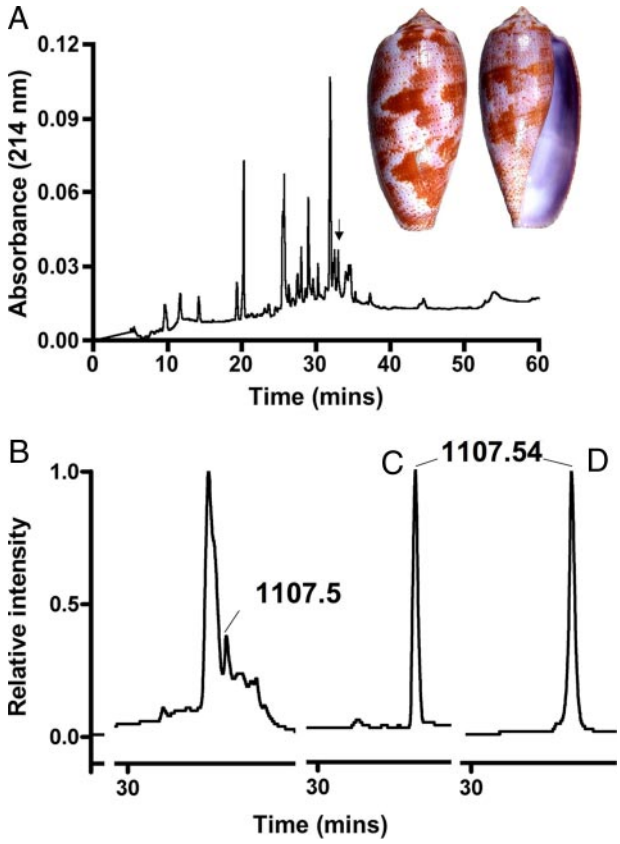

FIGURE 1. **Purification of conopressin-T.** *A*, RP-HPLC chromatogram showing the complexity of crude *C. tulipa* venom. The *arrow* indicates conopressin-T with a shell of *C. tulipa* shown in *inset*. *B*, fraction 30 contains conopressin-T, a novel bioactive peptide with a molecular mass of 1107.5 Da. *C*, purification to homogeneity of native conopressin-T from fraction 30. *D*, co-elution of native and synthetic conopressin-T. Both peptides elute at indistinguishable times.

sequencing (data not shown) unambiguously confirmed the sequence of Con-T as CYIQNCLRV-NH_2.

Synthesis of Conopressin-T and L7P-Conopressin-T—Con-T and its analogues were synthesized on 4-methylbenzhydrylamine resin using solid-phase peptide synthesis *t*-butoxycarbonyl chemistry to further validate the primary sequence and allow characterization of its biological activity. Lyophilized crude peptides from HF cleavage were dissolved in 0.5% trifluoroacetic acid and analyzed on analytical C_{18} Phenomenex RP-HPLC column. The chromatograms and electrospray-MS revealed that the syntheses contained >90% of the expected products; consequently, the oxidation was carried out directly on the crude peptides following the conditions described under "Experimental Procedures." During synthesis, we noticed that the replacement of Leu^7 by Pro^7 had a marked effect on solubility. L7P-Con-T dissolved readily in oxidation buffer to 0.5 mg/ml, whereas Con-T aggregated instantly in this solvent. This difference suggested that a Leu or a Pro at position 7 significantly modified the physical properties of the peptides. Oxidized synthetic and native Con-T were indistinguishable when co-injected in a C_{18} Phenomenex analytical RP-HPLC column (Fig. 1*D*).

Conopressin-T and L7P-Conopressin-T Are Selective V_{1a} Receptor Antagonists—Con-T and L7P-Con-T were tested for their ability to displace radioligand from human AVP and OT receptors expressed in HEK and CHO cells (Fig. 2*A* and Table 1). Con-T showed the highest affinity for human OTR (K_i = 108 nM) and $V_{1a}R$ (K_i = 319 nM) and no detectable activity at V_{1b} and V_2 receptors at up to 10 μM peptide. In contrast, L7P-Con-T was 8-fold more potent than Con-T at the $V_{1a}R$ (K_i = 37 nM) but had similar affinity for OTR (K_i = 132 nM). L7P-Con-T was also found to have a weak effect at V_2R (K_i = 1.8 μM), whereas no displacement of radioligand was detected at the $V_{1b}R$ at up to 10 μM peptide. For comparison, we also tested the activity of conopressin-S (Con-S) across these receptors. Con-S does not bind to V_2R (up to 10 μM peptide), has similar affinity for OTR (K_i = 175 nM) but is less potent at V_{1a} (K_i = 827 nM). In contrast to Con-T and L7P-Con-T, Con-S binds with high affinity to $V_{1b}R$ (K_i = 8.3 nM), although the displacement of specific [^{3}H]AVP binding was incomplete (a 30–40% resistant component remained; see Fig. 2*A*). Therefore, conopressin-T, -S, and -L7P have distinct pharmacological profiles on human receptors, with the lack of effect of Con-T on radioligand binding to both V_{1b} and V_2 receptors being unique (supplemental Fig. 1).

The functional properties of Con-T and L7P-Con-T were investigated on CHO cells expressing human receptors (Fig. 2*B* and Table 2). Con-T did not stimulate phospholipase C activity in cells expressing $V_{1a}R$ at ≤10 μM peptide. However, Con-T at 10 μM showed partial agonist activity at the $V_{1b}R$ and OTR, producing 9 and 22% of AVP and OT maximal activity, respectively. L7P-Con-T displayed a similar profile, with no agonist activity at the $V_{1a}R$ at ≤10 μM and partial agonist activity at the $V_{1b}R$ and OTR (4 and 28% of AVP and OT maximal activity, respectively) at 10 μM peptide. In contrast, both Con-T and L7P-Con-T induced a potent and concentration-dependent inhibition of AVP-stimulated IP production in CHO cells expressing $V_{1a}R$, with K_{inact} values of 329 and 90 nM, respectively (Table 2). These values correlated well with the binding affinities. Thus, both peptides are full antagonists at the human $V_{1a}R$ subtype and weak partial agonists for the $V_{1b}R$ and OTR (Fig. 2*B*). Due to the absence of significant binding to V_2R, the functional activity of Con-T and L7P-Con-T was not investigated on this subtype.

Gly^9 → Val Replacement in OT and AVP Acts as an Antagonist Switch at the V_{1a} Receptor—L7P-conopressin-T and vasotocin differs only at position 9, yet L7P-conopressin-T acts as a full antagonist at the V_{1a} receptor (Fig. 2*B*), whereas the closely related vasotocin is known to function as an agonist (29). To investigate if the Val^9 modification in conopressin-T could switch agonist to antagonist activity in related peptides, we tested this modification in OT and AVP. First, the binding properties of these analogues were assessed on human receptors (Fig. 3*A* and Table 1). G9V-AVP was equipotent at $V_{1a}R$ and V_2R (~25 nM) and 5–7-fold less potent at the OTR and $V_{1b}R$ (114 and 170 nM, respectively). Compared with AVP, G9V-AVP affinity ranged from 5-fold less at V_2R to 2000-fold less at $V_{1b}R$. In contrast, G9V-OT was equipotent at the V_{1a} and OT receptors (~465 nM), whereas it was unable to fully displace radioligands at the V_{1b} and V_2 subtypes at concentrations up to 10 μM. Compared with OT, G9V-OT affinity ranged from 13-fold less at $V_{1a}R$ to 309-fold less at OTR.

The functional properties of G9V-AVP and G9V-OT were investigated on CHO cells expressing human receptors (Fig. 3*B*

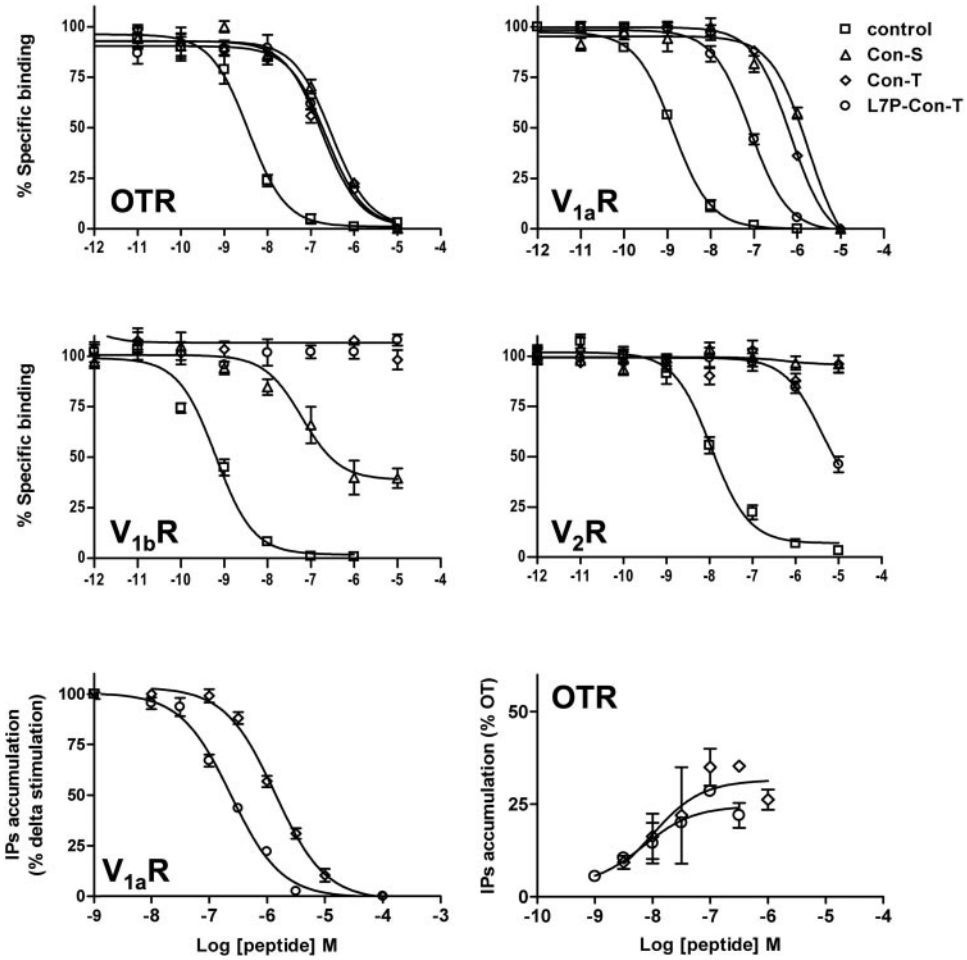

FIGURE 2. **Binding and functional properties of Con-T and L7P-Con-T on human vasopressin and oxytocin receptors.** *A*, Con-T (◇), Con-S (△), and L7P-Con-T (○) displacement of radioligands from OT, V_{1a}, V_{1b}, and V_2 receptors expressed in CHO cells. Control peptides were oxytocin (□) for the OTR and vasopressin (□) for all AVP receptors. *B*, functional properties of Con-T (◇) and L7P-Con-T (○) on human receptors. CHO cells stably transfected with V_{1a}R (*A*) or OTR (*B*) were grown in myo-[2-^{3}H]inositol medium and IP accumulation measured and expressed as a percentage of levels stimulated by AVP and OT. Results are the mean ± S.E. of three separate experiments, each performed in triplicate.

TABLE 1

Binding affinities (K_i, nM) on human vasopressin and oxytocin receptors

Compound	V_{1a}R	V_{1b}R	V_2R	OTR
Con-T	319 ± 15	>10,000	>10,000	108 ± 9
L7P-Con-T	37 ± 2	>10,000	1836 ± 392	132 ± 10
Con-S	827 ± 76	8.3 ± 1.6	>10,000	175 ± 13
AVP	0.6 ± 0.02	0.085 ± 0.01	4.9 ± 0.32	110 ± 25
G9V-AVP	25 ± 2	170 ± 22	24 ± 3	114 ± 35
OT	37 ± 3	222 ± 22	823 ± 122	1.5 ± 0.42
G9V-OT	466 ± 43	>10,000	>10,000	464 ± 171

Values are mean ± S.E. obtained from at least three separate experiments, each performed in triplicate.

and Table 2). Both peptides failed to stimulate phospholipase C activity in cells expressing V_{1a}R at ≤10 μM peptide. However, G9V-AVP and G9V-OT both acted as partial agonists at the OTR, eliciting ~5–10% and ~25–30% of OT maximal activity, respectively. In contrast, both peptides induced a potent and concentration-dependent inhibition of AVP-stimulated IP production in CHO cells expressing V_{1a}R. The affinities (K_{inact}) of G9V-AVP (40 nM) and G9V-OT (391 nM) correlate well with the binding data at the V_{1a} receptor (25 and 466 nM, respectively). Clearly, the G9V replacement shifted the activity of both AVP and OT from full agonist to full antagonist at the V_{1a}R, supporting the hypothesis that position 9 can act as a functional switch at the V_{1a} receptor.

Solution Structure of Con-T and L7P-Con-T—NMR spectral assignments of both peptides were made using established techniques (26). The chemical shifts in the amide region are well dispersed, and restraints derived from the NOESY spectra allowed determination of well defined structures. Analysis of the nuclear Overhauser effects indicated that the proline residue in L7P-Con-T is predominantly in a *trans* conformation based on the strong nuclear Overhauser effects between the Hα of Cys^6 and the Hδs of Pro^7. In addition, there is evidence of a minor conformation in the L7P-Con-T spectra, including a second proline spin system. However, this minor conformation could not be assigned because of its low intensity and missing peaks. It is not uncommon for small peptides to have prolines adopting mixed *cis/trans* conformations, which probably explains the second spin system observed.

The three-dimensional structures of conopressin-T and its L7P analogue were calculated using a simulated annealing protocol in CNS. The resulting families of structures had good structural and energetic statistics, as shown in Table 3. An ensemble of the 20 lowest energy structures for each peptide is shown in Fig. 4*A*. Analysis of the structures of each peptide with PROMOTIF (24) indicated that the major structural feature is a β-turn between residues 4 and 7. The structures of conopressin-T and L7P overlaid well over the defined regions of the structure (root mean square deviation for the backbone atoms of residues 1–6 is 0.52 Å). Although the C-terminal residues are disordered, the directions of the C-terminal tails clearly differ between the two structures as shown in Fig. 4, *B* and *C*.

DISCUSSION

Con-T isolated from *C. tulipa* venom is a novel vasopressin-like peptide. Investigation of its biological activity on human receptors revealed that Con-T acted selectively at V_{1a} and OT receptors. Functional studies demonstrated that Con-T was a full antagonist at V_{1a}R and a partial agonist at OTR. The pharmacological profile of an L7P analogue was similar but for increased affinity for the V_{1a}R. The partial agonist activity of both peptides at OTR indicates incomplete signaling through

TABLE 2
Antagonist and agonist actions of Con-T, L7P-Con-T, G9V-AVP, and G9V-OT on IP signaling through human vasopressin and oxytocin receptors

Compound	$V_{1a}R$	$V_{1b}R$	OTR
Con-T	No agonist activity at 10 μM (1 ± 7% of AVP maximum activity)	Weak agonist activity (9 ± 3% of AVP max activity at 10 μM)	Partial agonist (22 ± 3% of OT maximum activity; K_{act} 37 ± 30 nM)
	Antagonist, K_{inact} 329 ± 58 nM	No antagonist activity at 10 μM	No antagonist activity at 10 μM
L7P-Con-T	No agonist activity at 10 μM	Weak agonist activity at 10 μM (4 ± 2% of AVP max activity)	Partial agonist (28 ± 3% of OT max activity; K_{act} = 16 nM)
	Antagonist, K_{inact} 90 ± 12 nM	No antagonist activity at 10 μM	No antagonist activity at 10 μM
G9V-AVP	No agonist activity at 10 μM		Partial agonist (5–10% of OT maximum activity; K_{act} 320 ± 145 nM)
	Antagonist, K_{inact} 40 ± 10 nM	ND[a]	No antagonist activity at 10 μM
G9V-OT	No agonist activity at 10 μM		Partial agonist (25–30% of OT maximum activity; K_{act} 124 ± 37 nM)
	Antagonist, K_{inact} 391 ± 85 nM	ND	No antagonist activity at 10 μM

[a] ND, not determined.

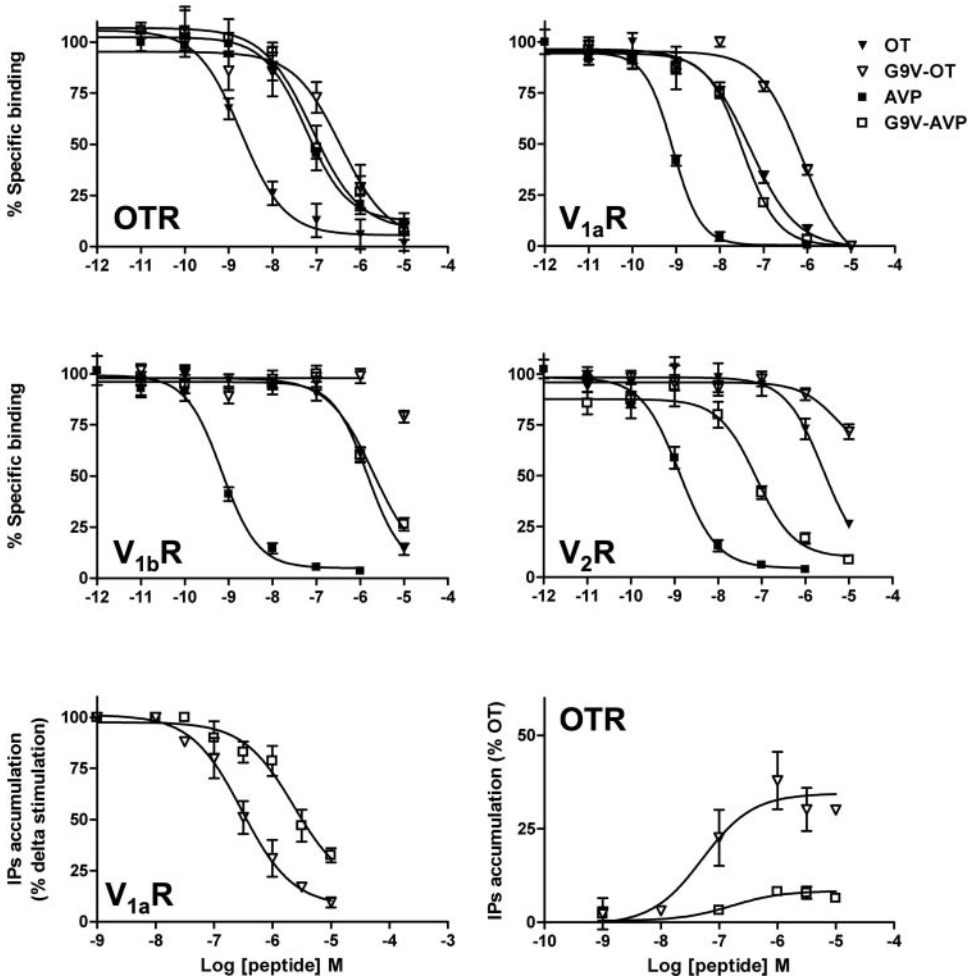

FIGURE 3. **Binding and functional properties of G9V-OT and G9V-AVP on human receptors.** *A*, G9V-AVP (□) and G9V-OT (▽) displacement of radioligands from OT, V_{1a}, V_{1b}, and V_2 receptors expressed in CHO cells. Control peptides were oxytocin (▼) and vasopressin (■) for all human receptors. *B*, functional properties of G9V-OT (▽) and G9V-AVP (□) on human receptors. CHO cells stably transfected with V_{1a}R (*left*) or OTR (*right*) were grown in myo-[2-^{3}H]inositol medium, and IP accumulation was measured and expressed as a percentage of levels stimulated by AVP and OT. The results are the mean ± S.E. of three separate experiments, each performed in triplicate.

the associated G protein ($G_{q/11}$, $G_{i/o}$) perhaps because they bind and trap the OT receptor in a conformation that is unable to signal fully. Similarly, OT and AVP act as partial agonists on vasopressin and oxytocin receptors, respectively (27).

The sequence of Con-T differs significantly from the previously reported conopressin-G and Con-S. First, the additional positively charged residue at position 4, which was thought to be characteristic of conopressins, is absent in Con-T. Interestingly, and probably ecologically and evolutionary relevant, Con-T has 7 of 9 residues (including the disulfide containing ring) identical to vasotocin, the teleost fish equivalent. In light of our pharmacological results, and since *C. tulipa* preys on fish, Con-T might specifically target teleost AVT receptors. So far, the only cloned receptor in teleost fish appears to be pharmacologically comparable with the mammalian V_{1a} and oxytocin receptors (28). This receptor controls the arterial-venous flows and is particularly important in gill hemodynamics and consequently respiration. However, conopressin-G and Con-S were found to be only moderately active on fish vasotocin receptor (29). Animal toxins usually shut down vital functions by blocking membrane receptors rather than by activating them, and although Con-T is yet to be tested on this fish receptor, it may act as an antagonist as demonstrated here for the human V_{1a} receptor. Alternatively, Con-T may also act synergistically with other lethal peptides present in the venom and/or modify the behavior of the fish to reduce the risk of injury to the cone snail. Interestingly, specific localization of staining for vasotocin in the brain of zebrafish was found to correlate with aggressive behavior (dominant *versus* subordinate social status) (30), and an antagonist might be expected to reduce such behavior. Other conopeptides are known to act centrally in fish, which have a leaky blood-brain barrier (31).

Recently, an unusual γ-carboxyglutamate at position 8 in the sequence of conopressin-Vil from the venom of *Conus villepinii*

TABLE 3
NMR and refinement statistics for conopressin-T and L7P-conopressin-T

	Conopressin-T	L7P-Conopressin-T
NMR distance and dihedral constraints		
Total NOE	49	42
Intraresidue	5	5
Sequential ($\|i - j\| = 1$)	30	26
Medium range ($\|i - j\| < 4$)	12	10
Long range ($\|i - j\| > 5$)	2	1
ϕ restraints	7	
Structure Statistics		
Violations (mean and S.D.)		
Distance constraints (Å)	0.06 ± 0.004	0.06 ± 0.016
Dihedral angle constraints (degrees)	0.49 ± 0.43	0.20 ± 0.22
Maximum dihedral angle violation (degrees)	3	3
Maximum distance constraint violation (Å)	0.3	0.3
Deviations from idealized geometry		
Bond lengths (Å)	0.004 ± 0.0001	0.004 ± 0.0005
Bond angles (degrees)	0.52 ± 0.03	0.47 ± 0.06
Impropers (degrees)	0.37 ± 0.07	0.36 ± 0.07
Average pairwise root mean square deviation[a] (Å)		
Backbone atoms (residues 1–6)	0.34 ± 0.14	0.55 ± 0.28
Heavy atoms (residues 1–6)	1.68 ± 0.45	1.61 ± 0.38

[a] Pairwise root mean square deviation was calculated among 20 refined structures.

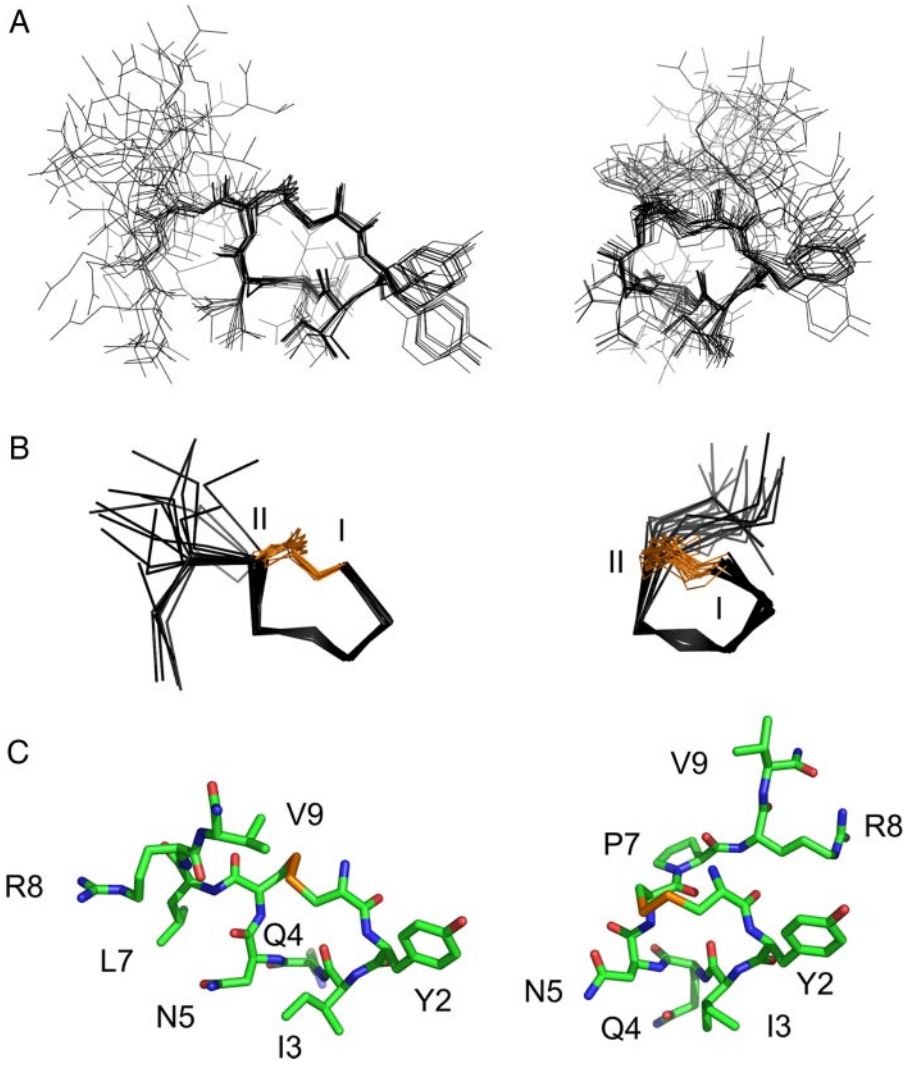

FIGURE 4. **Three-dimensional structures of Con-T (*left*; BMRB code 2007) and L7P-Con-T (*right*; BMRB code 2008).** *A*, superimposition of the 20 lowest energy structures. *B*, *ribbon representation* showing the backbone trace and cysteine connectivity (*yellow*). *C*, *stick representation* for each representative structure.

has been reported, but its biological activity was not determined (32). The discovery of multiple conopressin sequences supports the theory that the scaffold of the original vasopressin-like endogenous peptide in *Conus* has evolved for more specialized use in the venom (14).

Finally, the exocyclic tripeptide of Con-T has a Leu in position 7 and a Val in position 9. To our knowledge, Con-T is the first naturally occurring vasopressin-like peptide with substitutions at these positions (Table 4). Although substitutions within the tocin ring and at position 8 have been largely investigated over the past 50 years using natural and nonnatural amino acids, there has been limited study on positions 7 and 9, probably because of their absolute conservation in this peptide family. AVT acts as an agonist on AVP receptors (33), and since L7P-Con-T differs from AVT only at position 9 and acts as a V_{1a} antagonist, it appears that modification at this position alone can switch peptide activity from agonist to antagonist. In support of this hypothesis, the modification G9V in OT and AVP indeed switched their activity to a full antagonist at the V_{1a} receptor. Thus, all endogenous peptides in the AVP-like family have a Gly^9 (see Table 4) and act as agonists on their respective receptors, whereas

TABLE 4
Vasopressin-like peptide family

Name	Sequence	Species or phylum
Conopressin-T	CYIQNCLRV*[a]	*C. tulipa*
Conopressin-Vil	CLIQDCPγG*	*C. villepinii*
Conopressin-S	CIIRNCPRG*	*C. striatus*
Conopressin-G	CFIRNCPKG*	*C. geographus/imperialis*
Diuretic hormone	CLITNCPRG*	Locust (Insect)
Vasotocin	CYIQNCPRG*	Nonmammalian vertebrates
Phenypressin	CFFQNCPRG*	Marsupials
Lys-vasopressin	CYFQNCPKG*	Mammals (pigs)
Vasopressin	CYFQNCPRG*	Mammals
Cephalotocin	CYFRNCPIG*	*O. vulgaris*
Annetocin	CFVRNCPTG*	*E. foetida*
Glumitocin	CYISNCPQG*	Cartilaginous fishes
Valitocin	CYINNCPVG*	Cartilaginous fishes
Aspargtocin	CYINNCPLG*	Cartilaginous fishes
Phasvatocin	CYFNNCPVG*	Cartilaginous fishes
Mesotocin	CYIQNCPIG*	Lungfishes, marsupials
Isotocin	CYISNCPIG*	Osteichthyes
Oxytocin	CYIQNCPLG*	Mammals

[a] An asterisk indicates an amidated C-terminal. γ represents a γ-carboxyglutamate. The double underline represents conserved residues. The single underline represents conserved residues in all vasopressin-like peptides except in Con-T or Con-Vil.

Con-T, L7P-Con-T, G9V-OT, G9V-AVP, and a synthetic OT analogue with a Tyr^9 (34) act as antagonists. In contrast, all Val^9-containing peptides investigated here acted as partial agonists at the OT receptor.

The three-dimensional structures of conopressin-T and its L7P analogue were determined using NMR spectroscopy. Although the peptides are only 9 residues in length, well defined structures were determined for residues 1–6, presumably as a result of the constraints imposed by the disulfide bond between Cys^1 and Cys^6. The C-terminal regions are disordered but are oriented differently between the two peptides, indicating that Leu^7 has a significant influence on the overall structure of conopressin-T. This structural shift probably contributes to the relatively poor solubility of Con-T. Given that the orientation of the exocyclic residues is influenced by Pro^7, it appears that this relatively short stretch of peptide acts independently to determine peptide activity, since the pharmacological profiles of Con-T and L7P-Con-T are somewhat similar.

Comparison of the Con-T and L7P-Con-T structures with oxytocin and vasopressin highlights the similarity between all of the structures (supplemental Fig. 2). In particular, the loop between the two cysteine residues is structurally similar, with root mean square deviations of less than 1.5 Å for all structures. The C-terminal tails of Con-T and L7P-Con-T, although somewhat disordered, do not overlay well with the tail region of vasopressin or oxytocin. The proline residue in L7P-Con-T is in a *trans* conformation, but there is evidence for a minor conformation that may originate from a *cis* proline isomer. The proline geometry in OT and AVP has been extensively studied, with small percentages (~10%) of *cis* isomers in the solution conformations of these molecules (35). This finding is consistent with the current study as the population of the minor conformation of L7P-Con-T is ~7% based on relative peak intensities. Previous studies have shown that a *cis/trans* conformational change plays a role in OT receptor binding and activation (36), but significant differences are not observed for the affinity of Con-T and L7P-Con-T for the OTR, suggesting that *cis/trans* isomerization is less important for the affinity of these peptides.

The V_{1a} receptor was recently reported to play a major role in spatial memory (37), heart hypertrophy (38), and hyperfiltration (39). Selective inhibition of this receptor subtype may therefore have important therapeutic applications. The antagonist action of conopressin-T, as well as the determination of its three-dimensional structure, offer novel insights into the structure-activity relationship within the vasopressin peptide family that may guide the synthesis of novel analogues modified at positions 7 and 9 toward the design of highly selective V_{1a} antagonists.

Acknowledgments—We thank Vera Boulay for technical assistance (IGF, France), Andreas Brust and Barbara Colless (Xenome Ltd., Brisbane, Australia) for the HF cleavage and analytical HPLC peptide quantification of the synthetic peptides, Marion Loughnan for the preparation and fractionation of Conus tulipa crude venom, Alun Jones for the MS-MS experiments, and Jin Ai-Hua and Gene Hopping for fruitful discussions.

REFERENCES

1. Birnbaumer, M. (2000) *Trends Endocrinol. Metab.* **11,** 406–410
2. Barberis, C., Mouillac, B., and Durroux, T. (1998) *J. Endocrinol.* **156,** 223–229
3. Treschan, T. A., and Peters, J. (2006) *Anesthesiology* **105,** 599–612; quiz 639–540
4. Febo, M., Numan, M., and Ferris, C. F. (2005) *J. Neurosci.* **25,** 11637–11644
5. Ferris, C. F., Lu, S. F., Messenger, T., Guillon, C. D., Heindel, N., Miller, M., Koppel, G., Robert Bruns, F., and Simon, N. G. (2006) *Pharmacol Biochem. Behav.* **83,** 169–174
6. Kozorovitskiy, Y., Hughes, M., Lee, K., and Gould, E. (2006) *Nat. Neurosci.* **9,** 1094–1095
7. Hoyle, C. H. (1999) *Brain Res.* **848,** 1–25
8. Cruz, L. J., de Santos, V., Zafaralla, G. C., Ramilo, C. A., Zeikus, R., Gray, W. R., and Olivera, B. M. (1987) *J. Biol. Chem.* **262,** 15821–15824
9. McMaster, D., Kobayashi, Y., and Lederis, K. (1992) *Peptides* **13,** 413–421
10. Salzet, M., Bulet, P., Van Dorsselaer, A., and Malecha, J. (1993) *Eur. J. Biochem.* **217,** 897–903
11. Van Kesteren, R. E., Smit, A. B., De Lange, R. P., Kits, K. S., Van Golen, F. A., Van Der Schors, R. C., De With, N. D., Burke, J. F., and Geraerts, W. P. (1995) *J. Neurosci.* **15,** 5989–5998
12. Fry, B. G. (2005) *Genome Res.* **15,** 403–420
13. Dutertre, S., Lumsden, N. G., Alewood, P. F., and Lewis, R. J. (2006) *FEBS Lett.* **580,** 3860–3866
14. Nielsen, D. B., Dykert, J., Rivier, J. E., and McIntosh, J. M. (1994) *Toxicon* **32,** 845–848
15. Lewis, R. J., Nielsen, K. J., Craik, D. J., Loughnan, M. L., Adams, D. A., Sharpe, I. A., Luchian, T., Adams, D. J., Bond, T., Thomas, L., Jones, A., Matheson, J. L., Drinkwater, R., Andrews, P. R., and Alewood, P. F. (2000) *J. Biol. Chem.* **275,** 35335–35344
16. Schnolzer, M., Alewood, P., Jones, A., Alewood, D., and Kent, S. B. (1992) *Int. J. Pept. Protein Res.* **40,** 180–193
17. Cheng, Y., and Prusoff, W. H. (1973) *Biochem. Pharmacol* **22,** 3099–3108
18. Derick, S., Cheng, L. L., Voirol, M. J., Stoev, S., Giacomini, M., Wo, N. C., Szeto, H. H., Ben Mimoun, M., Andres, M., Gaillard, R. C., Guillon, G., and Manning, M. (2002) *Endocrinology* **143,** 4655–4664
19. Daly, N. L., Ekberg, J. A., Thomas, L., Adams, D. J., Lewis, R. J., and Craik, D. J. (2004) *J. Biol. Chem.* **279,** 25774–25782
20. Rosengren, K. J., Daly, N. L., Plan, M. R., Waine, C., and Craik, D. J. (2003) *J. Biol. Chem.* **278,** 8606–8616
21. Guntert, P., Mumenthaler, C., and Wuthrich, K. (1997) *J. Mol. Biol.* **273,** 283–298
22. Brunger, A. T., Adams, P. D., and Rice, L. M. (1997) *Structure* **5,** 325–336
23. Linge, J. P., and Nilges, M. (1999) *J. Biomol. NMR* **13,** 51–59
24. Hutchinson, E. G., and Thornton, J. M. (1996) *Protein Sci.* **5,** 212–220
25. Laskowski, R. A., Rullmannn, J. A., MacArthur, M. W., Kaptein, R., and

Thornton, J. M. (1996) *J. Biomol. NMR* **8,** 477–486
26. Wuthrich, K. (1986) *NMR of Proteins and Nucleic Acids*, Wiley-Interscience, New York
27. Chini, B., Mouillac, B., Balestre, M. N., Trumpp-Kallmeyer, S., Hoflack, J., Hibert, M., Andriolo, M., Pupier, S., Jard, S., and Barberis, C. (1996) *FEBS Lett.* **397,** 201–206
28. Balment, R. J., Lu, W., Weybourne, E., and Warne, J. M. (2006) *Gen. Comp. Endocrinol* **147,** 9–16
29. Mahlmann, S., Meyerhof, W., Hausmann, H., Heierhorst, J., Schonrock, C., Zwiers, H., Lederis, K., and Richter, D. (1994) *Proc. Natl. Acad. Sci. U. S. A.* **91,** 1342–1345
30. Larson, E. T., O'Malley, D. M., and Melloni, R. H., Jr. (2006) *Behav. Brain Res.* **167,** 94–102
31. Adeyemo, O. M., Shapira, S., Tombaccini, D., Pollard, H. B., Feuerstein, G., and Siren, A. L. (1991) *Toxicol. Appl. Pharmacol* **108,** 489–496
32. Moller, C., and Mari, F. (2007) *Biochem. J.* **404,** 413–419
33. Kruszynski, M., Manning, M., Wo, N. C., and Sawyer, W. H. (1990) *Experientia* **46,** 771–773
34. Elands, J., Barberis, C., Jard, S., Tribollet, E., Dreifuss, J. J., Bankowski, K., Manning, M., and Sawyer, W. H. (1988) *Eur. J. Pharmacol.* **147,** 197–207
35. Larive, C. K., Guerra, L., and Rabenstein, D. L. (1992) *J. Am. Chem. Soc.* **114,** 7331–7337
36. Wittelsberger, A., Patiny, L., Slaninova, J., Barberis, C., and Mutter, M. (2005) *J. Med. Chem.* **48,** 6553–6562
37. Egashira, N., Tanoue, A., Higashihara, F., Mishima, K., Fukue, Y., Takano, Y., Tsujimoto, G., Iwasaki, K., and Fujiwara, M. (2004) *Neurosci. Lett.* **356,** 195–198
38. Hiroyama, M., Wang, S., Aoyagi, T., Oikawa, R., Sanbe, A., Takeo, S., and Tanoue, A. (2007) *Eur. J. Pharmacol.* **559,** 89–97
39. Windt, W. A., Tahara, A., Kluppel, A. C., de Zeeuw, D., Henning, R. H., and van Dokkum, R. P. (2006) *J. Renin. Angiotensin Aldosterone Syst.* **7,** 217–224